

# Physical origin of satellites in photoemission of doped graphene: an *ab initio* GW plus cumulant study

Johannes Lischner, Derek Vigil-Fowler, and Steven G. Louie  
*Department of Physics, University of California, Berkeley,  
 California 94720, USA, and Materials Sciences Division,  
 Lawrence Berkeley National Laboratory, Berkeley 94720, USA.*

We calculate the photoemission spectra of suspended and epitaxial doped graphene using an *ab initio* cumulant expansion of the Green's function based on the GW self-energy. Our results are compared to experiment and to standard GW calculations. For doped graphene on a silicon carbide substrate, we find, in contrast to earlier calculations, that the spectral function from GW only does not reproduce experimental satellite properties. However, *ab initio* GW plus cumulant theory combined with an accurate description of the substrate screening results in good agreement with experiment, but gives no plasmaron (i.e., no extra well-defined excitation satisfying Dyson's equation).

**Introduction.**—The isolation of graphene [1], an atomically thin layer of carbon, in 2004 has sparked much interest and an enormous amount of scientific work. Among the most fascinating properties of this extraordinary material is its electronic structure: the low energy valence and conduction bands form two Dirac cones in the Brillouin zone causing electrons in graphene to behave like massless relativistic particles with chiral character.

Recently, several experimental groups probed the low-energy electronic structure of doped graphene on a silicon carbide (SiC) substrate using angle-resolved photoemission spectroscopy (ARPES) [2–4]. Surprisingly, the experimental spectra did not exhibit simple Dirac cones, but indicated a more complicated electronic structure. There has been much discussion regarding the interpretation of the observed findings: while Lanzara and coworkers [4] concluded that the SiC substrate induces a band gap in graphene, Rotenberg and coworkers [2, 3] argued that the observed electronic structure is intrinsic to graphene and is due to a *plasmaron* excitation caused by strong electron-carrier plasmon coupling.

Both interpretations were backed by theoretical findings: Kim et al. [5] carried out density-functional calculations of graphene on a reconstructed SiC surface and found that the dangling bonds of the substrate bind to the graphene layer breaking the symmetry of the graphene sheet and causing a band gap to open. On the other hand, Polini et al. [6] and Hwang and Das Sarma [7] carried out Green's function calculations on the Dirac Hamiltonian (model system with two linear bands) using the GW approximation [8] to the self-energy and a simplified description of the substrate. These calculations found strong low-energy plasmaronic bands which obey the experimentally observed scaling law as a function of doping, and Bostwick *et al.* reported agreement of theory with experiment after introducing an adjustable parameter attributed to the SiC substrate screening[3].

The agreement of GW calculations and experiment for satellite properties in doped graphene is surprising since

it is known that for bulk solids, such as silicon or potassium [9–11], electron correlations *beyond the GW approximation* are needed to accurately describe plasmon satellites. For bulk solids, the GW plus cumulant (GW+C) approximation [10, 11], which includes significant vertex corrections, provides an accurate description of plasmon satellites, but does not find plasmarons. However, no application of the GW+C theory to a two dimensional system, such as doped graphene with its characteristic low-energy carrier plasmon, has been reported so far. Also, in contrast to bulk solids, the carrier plasmon dispersion in graphene is *tunable* and is both substrate and doping dependent.

In this Letter, we investigate satellites in photoemission spectra of doped suspended graphene and doped graphene on a SiC substrate using the *ab initio* cumulant expansion of the Green's function based on the GW approximation to the self-energy. We compare our findings with those from *ab initio* GW calculations and also with GW calculations based on the model Dirac Hamiltonian. As a benchmark, we also calculated *ab initio* GW+C photoemission spectra for silicon.

**Methods.**—The photoelectron current in an ARPES experiment with monochromatic photons of frequency  $\nu$  and polarization  $\hat{e}_\nu$  is given by [12]

$$I(\mathbf{k}, \omega, \hat{e}_\nu, \nu) = \sum_n^{\text{occ}} I_0(n, \mathbf{k}, \omega, \hat{e}_\nu, \nu) f(\omega) A_{n\mathbf{k}}(\omega), \quad (1)$$

where  $\mathbf{k}$  and  $\omega$  are the momentum and binding energy of an electron in band  $n$ ,  $f(\omega)$  is the Fermi-Dirac distribution and  $I_0$  includes the absorption cross section of the incident photons. Also,  $A_{n\mathbf{k}}(\omega) = 1/\pi |\text{Im} G_{n\mathbf{k}}(\omega)|$  denotes the spectral function with  $G_{n\mathbf{k}}(\omega)$  being the interacting one-particle Green's function.

Usually,  $G_{n\mathbf{k}}(\omega)$  is obtained by solving Dyson's equation  $G_{n\mathbf{k}}^{-1}(\omega) = G_{0,n\mathbf{k}}^{-1}(\omega) - \Sigma_{n\mathbf{k}}(\omega) + V_{n\mathbf{k}}^{xc}$  with  $G_{0,n\mathbf{k}}(\omega)$  and  $V_{n\mathbf{k}}^{xc}$  denoting a mean-field Green's function and exchange-correlation potential, respectively, and  $\Sigma_{n\mathbf{k}}(\omega)$  is the self-energy. In this work, we employ the *ab initio*

GW approach to the self-energy [8, 13].

While describing quasiparticle properties in many materials with high accuracy [13], the GW approximation is less reliable for satellite properties [9–11]: for the spectral function of a core electron interacting with plasmons, GW predicts a single satellite instead of a satellite series with decreasing spectral weight and also greatly overestimates the binding energy of the satellite structures. The cumulant expansion [10, 14, 15] of  $G_{n\mathbf{k}}(\omega)$  cures these deficiencies by including significant vertex corrections beyond GW: it provides the *exact* solution for a core electron interacting with plasmons [9]. In the cumulant approach, the Green's function for a hole is expressed as

$$G_{n\mathbf{k}}(t) = i\Theta(-t)e^{-i\epsilon_{n\mathbf{k}}t + C_{n\mathbf{k}}(t)}, \quad (2)$$

where  $\epsilon_{n\mathbf{k}}$  denotes the mean-field orbital energy and  $C_{n\mathbf{k}}(t)$  denotes the cumulant. This expression for the Green's function is obtained after the first iteration of the self-consistent solution of its equation of motion assuming a simple quasiparticle form for the starting guess [14].

The cumulant can be separated into a quasiparticle part  $C_{n\mathbf{k}}^{qp}(t)$  and a satellite part  $C_{n\mathbf{k}}^{sat}(t)$  given formally in terms of the self-energy by (for  $t < 0$ )

$$C_{n\mathbf{k}}^{qp}(t) = -it\Sigma_{n\mathbf{k}}(E_{n\mathbf{k}}) + \frac{\partial \Sigma_{n\mathbf{k}}^h(E_{n\mathbf{k}})}{\partial \omega} \quad (3)$$

$$C_{n\mathbf{k}}^{sat}(t) = \frac{1}{\pi} \int_{-\infty}^{\mu} d\omega \frac{\text{Im}\Sigma_{n\mathbf{k}}(\omega)}{(E_{n\mathbf{k}} - \omega - i\eta)^2} e^{i(E_{n\mathbf{k}} - \omega)t}, \quad (4)$$

where  $\mu$  denotes the chemical potential,  $\eta$  is a positive infinitesimal,  $E_{n\mathbf{k}} = \epsilon_{n\mathbf{k}} + \Sigma_{n\mathbf{k}}(E_{n\mathbf{k}}) - V_{n\mathbf{k}}^{xc}$  is the quasiparticle energy and  $\Sigma_{n\mathbf{k}}^h(\omega)$  is defined through the relation

$$\Sigma_{n\mathbf{k}}^h(\omega) = \frac{1}{\pi} \int_{-\infty}^{\mu} d\omega' \frac{\text{Im}\Sigma_{n\mathbf{k}}(\omega')}{\omega' - \omega - i\eta}. \quad (5)$$

For a given level of approximation for  $\Sigma$ , the cumulant theory yields an improved Green's function through Eqs. (2-5). In the present study,  $\Sigma$  is obtained from *ab initio* GW theory [13] which is known to describe quasiparticle properties in Si, C and related materials accurately thus providing a good starting point for the cumulant theory.

*Silicon.*—To benchmark the accuracy of the *ab initio* GW+C approach, we first applied it to silicon where accurate angle-integrated photoemission data is available [11]. We carried out one-shot full frequency  $G_0W_0$  calculations for  $\Sigma$  using the BerkeleyGW package[16] [see Supplementary Materials (SM) for details] and then evaluated the cumulant spectral function.

The inset of Fig. 1 compares the spectral functions from *ab initio* GW and *ab initio* GW+C theory for the lowest valence band at the  $\Gamma$  point of silicon. While the GW spectral function exhibits a strong plasmaron peak

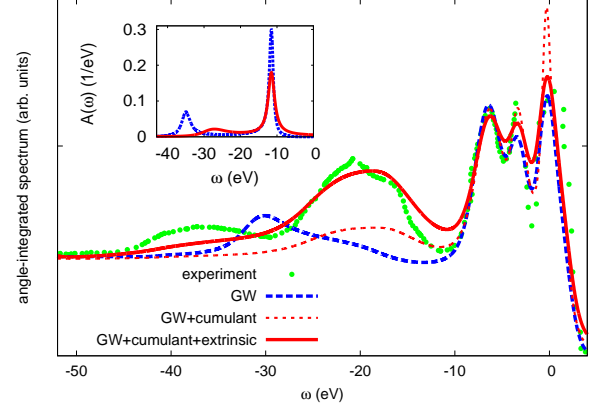


FIG. 1: Comparison of theoretical results and experiment data[11] for the angle-integrated photoemission spectrum of silicon. The inset shows the spectral function of the lowest valence band at the  $\Gamma$ -point ( $\Gamma_{1v}$ ) in silicon from *ab initio* GW (dashed blue curve) and *ab initio* GW+C (solid red curve) theories. The energy is measured from the top of the valence band

due to an additional spurious solution of Dyson's equation [9–11] (see SM) separated by  $\sim 23$  eV from the quasiparticle peak, the GW+C spectral function shows a more shallow peak separated by  $\sim 16$  eV from the quasiparticle peak. This separation agrees well with the experimental plasmon energy of 16.6 eV [17] in silicon indicating a much weaker interaction between electrons and plasmons than predicted by GW.

Figure 1 shows the angle-integrated photoemission spectrum from the *ab initio* GW+C theory and compares it to the *ab initio* GW result and experiment. We have included matrix element effects, the inelastic background and extrinsic plasmon losses similar to the work of Guzzo and coworkers [11] (see SM). Our full frequency *ab initio* GW+C theory reproduces accurately the location, height and width of the first plasmon peak and it does not show a significant second peak.

*Doped Graphene.*—In contrast to silicon where the plasmons are high-energy excitations, doped graphene exhibits a low-energy, dispersive plasmon branch due to added carriers from doping with a characteristic 2D square root of  $q$  dispersion relation [3, 6, 7], the so-called carrier plasmon. Due to the special dispersion relations of the carrier plasmons and of the Dirac fermions, the self-energy of doped graphene exhibits very sharp features in  $(\mathbf{k}, \omega)$ -space [6, 7] necessitating *extremely* fine k-point and frequency grids for convergent results: our calculation of  $\Sigma_{n\mathbf{k}}(\omega)$  and  $A_{n\mathbf{k}}(\omega)$  employs a full frequency sampling at 0.05 eV intervals and a  $1440 \times 1440 \times 1$  k-point grid (see SM).

Figure 2(a) shows the *ab initio* GW+C spectral function at the Dirac point of isolated graphene with electron doping resulting in a charge density  $n = -12.4 \times 10^{13} \text{ cm}^{-2}$ . Also shown are the *ab initio* GW spectral

function and the GW spectral function from the linear-band model[6, 7]. (In the linear-bands model, graphene is described by the Dirac Hamiltonian with a bandstructure consisting of only two linear bands at the K and K' points of the Brillouin zone.) For the linear-band model, we included screening contributions from all other bands by adding the analytically parametrized cRPA dielectric function calculated within DFT by excluding the  $p_z$  bands, obtained by Wehling and coworkers (Eq. (3) of Ref.[18]), to the calculated dielectric function of the linear-band model [19, 20]. We verified the accuracy of the cRPA dielectric function of Wehling *et al.* by comparing it to the additional background dielectric constant  $\kappa(q)$  necessary to match the carrier plasmon peak of the imaginary part of the interacting susceptibility from the linear-band model to the corresponding peak in the *ab initio* calculation [see inset of Fig.2(b)].

Despite the simplification of the graphene band structure in the linear-band model, the resulting GW spectral function is similar to the *ab initio* GW result provided that the above  $\kappa(q)$  is used: both theories give a strong quasiparticle peak and a smaller satellite peak. The separation of the peaks is similar, 0.83 eV in *ab initio* GW and 0.89 eV in the linear-band model. However, the shapes of the features differ noticeably: in the *ab initio* GW theory, the quasiparticle peak is much broader than in the linear-band model, while the satellite peak is sharper revealing the importance of a realistic bandstructure for high doping levels. The GW approximation leads to a spurious plasmaron solution of Dyson's equation giving rise to the peak near -2 eV in Fig. 2(a) (see SM). The inclusion of higher order electron interaction effects in the *ab initio* GW+C calculations show important changes in the spectral function in Fig. 2: i) there is a significant shift of the amplitude from the quasiparticle peak to the satellite peak, and ii) the peak separation is reduced to 0.62 eV, a change of  $\sim 30$  percent. The inset in Figure 2(a) shows that the *ab initio* GW+C spectral function also exhibits an additional shoulder-like structure at  $\omega \sim -2.3$  eV resulting from the coupling of the hole to two plasmons. So far no experimental ARPES spectrum with sufficient accuracy to observe satellite features has yet been reported for suspended graphene.

Bostwick and coworkers had carried out ARPES experiments on hydrogen-intercalated epitaxial graphene grown on SiC(0001) [3, 22]. To include the screening effect of the substrate we model the substrate by a 10-atomic-layer thick slab of hydrogen-terminated 4H-SiC(0001) employing the  $\sqrt{3} \times \sqrt{3}R30^\circ$  SiC surface unit cell [23–25] [see inset of Figure 3(b)] resulting in a supercell geometry with neighboring graphene sheets separated by 54 a.u.. To determine the SiC-graphene distance we carried out density-functional theory calculations with the empirical van der Waals correction of Grimme [26] and obtain a separation of 3.86 Å which agrees well with the findings of Soltys and coworkers [25].

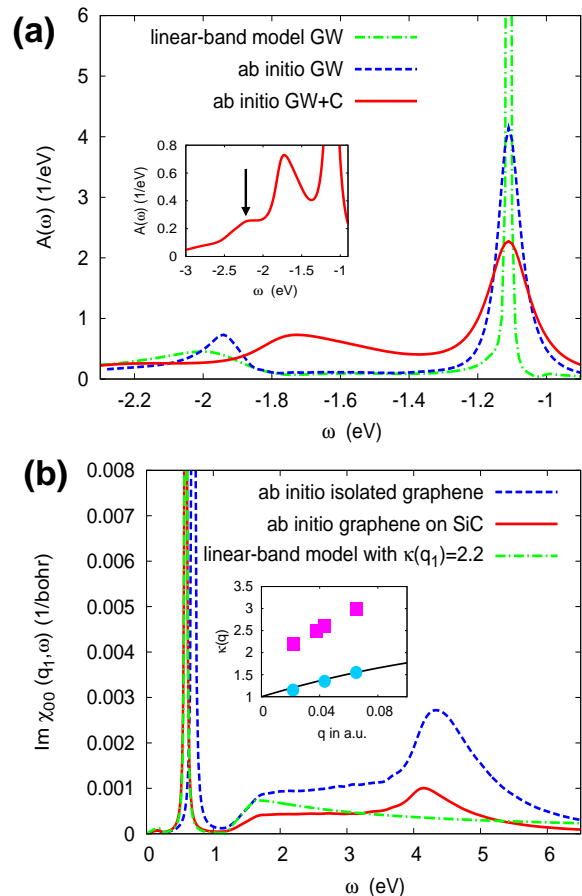


FIG. 2: (a): Comparison of *ab initio* GW+C, *ab initio* GW, and linear-band model GW spectral functions at the Dirac point for isolated graphene with electron doping corresponding to a charge density  $n = -12.4 \times 10^{13} \text{ cm}^{-2}$ . Energies are measured relative to the Fermi energy. The inset shows an additional shoulder-like feature (indicated by arrow) in the *ab initio* GW+C spectral function. (b): Imaginary part of the head of the interacting susceptibility (in a supercell calculation  $\text{Im}\chi_{00}(\mathbf{q}, \omega) = \text{Im}\epsilon_{00}^{-1}(\mathbf{q}, \omega)/v(\mathbf{q})/n_g$  with  $v(\mathbf{q})$  denoting the truncated Coulomb interaction and  $n_g$  the density of graphene sheets per unit length) for isolated graphene and for graphene on a SiC substrate. Note that  $\text{Im}\chi_{00}(\mathbf{q}, \omega)$  is proportional to the dynamical structure factor  $S(\mathbf{q}, \omega)$  [21]. We also show the result from the linear-band model with a background dielectric of  $\kappa(q_1) = 2.2$ . The results are for  $n = -5.9 \times 10^{13} \text{ cm}^{-2}$  and  $q_1 = 0.022 \text{ a.u.}$ . The inset shows the background dielectric function  $\kappa(q)$  used in the strictly 2D linear-band model for isolated graphene (solid circles), graphene on SiC (solid squares) and the cRPA result for isolated graphene obtained by Wehling *et al.* (solid line)[18].

Because of the passivation of the surface dangling bonds by hydrogen atoms, we also do not find a surface induced band gap opening in the graphene sheet [25].

We then carried out GW calculations on the graphene+substrate system using a truncated Coulomb interaction [16]. Due to the immense size of the system under consideration, we separately calculate the contri-

butions to the polarizability matrix from the graphene sheet and the substrate before adding them up (see SM).

Figure 2(b) shows the imaginary part of the interacting susceptibility of graphene on H-passivated SiC for  $n = -5.9 \times 10^{13} \text{ cm}^{-2}$  at a small wave vector  $q_1 = 0.022 \text{ a.u.}$  and compares it to the isolated graphene result. The substrate screening leads to a reduction of the carrier plasmon frequency (the position of the sharp peak at  $\sim 0.7 \text{ eV}$ ). Figure 2(b) also shows that the plasmon peak of the linear-band model coincides with the *ab initio* result if the 2D bare Coulomb interaction is divided by a background dielectric constant  $\kappa(q_1) = 2.2$  which now contains both the intrinsic graphene screening processes discussed earlier and screening contributions from the substrate. This deduced *ab initio* value of  $\kappa$  is much smaller than the value used by Bostwick and coworkers [3] who treated  $\kappa$  as a *q-independent fitting parameter* and found that  $\kappa = 5.15$  (using the LDA Fermi velocity to convert the coupling strength  $\alpha_G = 0.5$  to a background dielectric constant) gives the best description of the experimental spectra within the GW approximation only. We find that  $\kappa$  increases with  $q$ , but remains much smaller than the value needed by Bostwick and coworkers to fit experiment [see inset of Fig. 2(b)].

Figure 3(a) compares *ab initio* GW+C and GW spectral functions for graphene on SiC at the Dirac point with experiment for  $n = -5.9 \times 10^{13} \text{ cm}^{-2}$ . All spectral functions exhibit a quasiparticle peak and a satellite: their separation is  $0.44 \text{ eV}$  in GW and  $0.27 \text{ eV}$  in the GW+C theory. The *ab initio* GW+C theory agrees very well with the experimental separation of  $0.30 \text{ eV}$  [3]. Also, the shape of the GW+C spectral function resembles the experimental spectrum more closely than the GW result. The inset of Fig. 3(a) shows that GW predicts an additional plasmaron solution to Dyson's equation. In contrast, no plasmaron solution is found if the vertex-corrected self-energy  $\delta\Sigma_{GW+C} = G_0^{-1} - G_{GW+C}^{-1}$  is used. We attribute the remaining difference between the experimental spectrum and the computed spectral function to extrinsic losses (i.e., emission of plasmons by the photoexcited electron), which are not included in our theory (see SM for a preliminary treatment of extrinsic losses).

Bostwick and coworkers have shown that the experimental spectral functions exhibit an important scaling behavior as function of doping [3]: when the experimental quasiparticle-satellite separation is divided by the Fermi level  $E_F$  the resulting number is independent of doping for a wide range of doping levels, a consequence of the linear dispersion of electrons in graphene. To check whether the *ab initio* GW+C method reproduces this scaling behavior we carried out calculations for  $n = -1.5 \times 10^{13} \text{ cm}^{-2}$ . The results are shown in Fig. 3(b). Again, we find that the separation of quasiparticle and satellite peaks is described accurately by the *ab initio* GW+C method.

In conclusion, we have carried out a first-principles

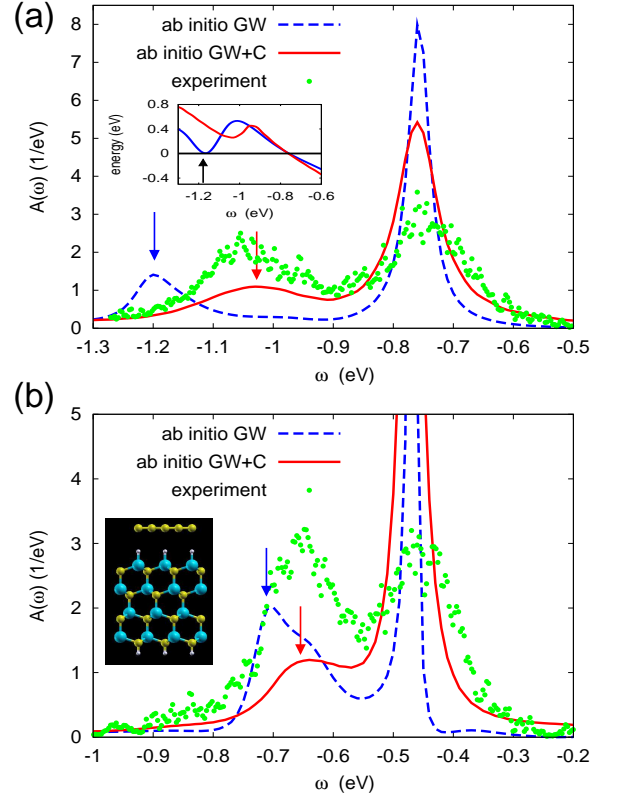


FIG. 3: Comparison of *ab initio* GW+C and GW spectral function (in  $1/\text{eV}$ ) for graphene on SiC at the Dirac point with experiment (experimental spectra are given in counts/second in arbitrary units) for (a)  $n = -5.9 \times 10^{13} \text{ cm}^{-2}$  and (b)  $n = -1.5 \times 10^{13} \text{ cm}^{-2}$ . The arrows indicate the satellite position in the theoretical curves. The inset of (a) shows  $\text{Re}\delta\Sigma(\omega) - \omega + \epsilon_{LDA}$  with  $\delta\Sigma = G_0^{-1} - G^{-1}$  for GW (blue curve) and GW+C (red curve) as a function of  $\omega$ . The arrow denotes the plasmaron solution in GW, which does not exist in GW+C. The inset of (b) shows the geometry of graphene on a hydrogen-terminated 4H-SiC (0001) surface: carbon atoms are brown, silicon atoms are blue and hydrogens are white.

study of doped graphene on hydrogen-intercalated SiC, going beyond standard GW calculations, which explains the experimental findings of Bostwick and coworkers [3]. The work reproduces the experimental satellite properties without finding a plasmaron showing the importance of an advanced treatment of electron correlations via the *ab initio* GW+C method and an accurate modelling of substrate screening. We do not find a substrate induced band gap or a plasmaron solution. We also explain the previously reported good fit of GW calculations to experiment using a simplified modelling of the substrate [3]. In these calculations, the lack of sufficient electron correlations at the GW level leads to an extra solution to Dyson's equation which gives rise to an overestimation of the quasiparticle-satellite separation. However, these calculations also overestimate the effect of substrate screening resulting in spurious agreement with experiment.

We acknowledge useful discussions with Allan MacDonald, Marco Polini, Alessandro Principi, Matteo Guzzo, Felipe da Jornada, Manish Jain, and Aaron Bostwick. We acknowledge support in our initial work formulating the conceptual foundations of this Letter and partial postdoctoral support for one of us (J.L.) from National Science Foundation Grant No. DMR10-1006184. We also acknowledge support in the computational part of this project and for student support (D.V.F.) from the Director, Office of Science, Office of Basic Energy Sciences, Materials Sciences and Engineering Division, U.S. Department of Energy under Contract No. DE-AC02-05CH11231. D.V.F. was also supported by a Department of Defense (DoD) National Defense Science & Engineering Graduate Fellowship. Computational resources have been provided by the DOE at Lawrence Berkeley National Laboratorys NERSC facility and by the NSF through XSEDE resources at NICS.

- 
- [1] K. S. Novoselov, A. K. Geim, S. V. Morozov, D. Jiang, Y. Zhang, S. V. Dubonos, I. V. Grigrieva, and A. A. Firsov, *Science* **306**, 666 (2004).
  - [2] E. Rotenberg, A. Bostwick, T. Ohta, J. L. McChesney, T. Seyller, and K. Horn, *Nature Materials* **7**, 258 (2008).
  - [3] A. Bostwick, F. Speck, T. Seyller, K. Horn, M. Polini, R. Asgari, A. H. MacDonald, and E. Rotenberg, *Science* **328**, 999 (2010).
  - [4] S. Y. Zhou, G.-H. Gweon, A. V. Fedorov, P. N. First, W. A. de Heer, D.-H. Lee, F. Guinea, A. H. C. Neta, and A. Lanzara, *Nature Materials* **6**, 770 (2007).
  - [5] S. Kim, J. Ihm, H. J. Choi, and Y.-W. Son, *Phys. Rev. Lett.* **100**, 176802 (2008).
  - [6] M. Polini, R. Asgari, G. Borghi, Y. Barlas, T. Peregr-Barnea, and A. H. MacDonald, *Phys. Rev. B* **77**, 081411(R) (2008).
  - [7] E. H. Hwang and S. D. Sarma, *Phys. Rev. B* **77**, 081412(R) (2008).
  - [8] L. Hedin and S. Lundqvist, *Solid State Physics* **23**, 1 (1970).
  - [9] D. C. Langreth, *Phys. Rev. B* **1**, 471 (1970).
  - [10] F. Aryasetiawan, L. Hedin, and K. Karlsson, *Phys. Rev. Lett.* **77**, 2268 (1996).
  - [11] M. Guzzo, G. Lani, F. Sottile, P. Romaniello, M. Gatti, J. J. Kas, J. J. Rehr, M. G. Silly, F. Sirotti, and L. Rein-ing, *Phys. Rev. Lett.* **107**, 166401 (2011).
  - [12] A. Damascelli, Z. Hussain, and Z.-X. Shen, *Rev. Mod. Phys.* **75**, 473 (2003).
  - [13] M. S. Hybertsen and S. G. Louie, *Phys. Rev. B* **34**, 5390 (1986).
  - [14] C.-O. Almbladh and L. Hedin, *Handbook of Synchrotron Radiation*, vol. 1 (E. E. Koch (North-Holland, Amsterdam), 1983).
  - [15] L. Hedin, *Physica Scripta* **21**, 477 (1980).
  - [16] J. Deslippe, G. Samsonidze, D. A. Strubbe, M. Jain, M. L. Cohen, and S. G. Louie, *Comput. Phys. Commun.* **183**, 1269 (2012).
  - [17] H. R. Philipp and H. Ehrenreich, *Phys. Rev.* **129**, 1550 (1963).
  - [18] T. O. Wehling, E. Şaşıoğlu, C. Friedrich, A. I. Liechtenstein, M. I. Katsnelson, and S. Blügel, *Phys. Rev. Lett.* **106**, 236805 (2011).
  - [19] E. H. Hwang and S. D. Sarma, *Phys. Rev. B* **75**, 205418 (2007).
  - [20] B. Wunsch, T. Stauber, F. Sols, and F. Guinea, *New J. Phys.* **8**, 318 (2006).
  - [21] E. H. Hwang, R. Sensarma, and S. D. Sarma, *Phys. Rev. B* **82**, 195406 (2010).
  - [22] C. Riedl, C. Coletti, T. Iwasaki, A. A. Zakharov, and U. Starke, *Phys. Rev. Lett.* **103**, 246804 (2009).
  - [23] F. Varchon, R. Feng, J. Hass, X. Li, B. N. Nguyen, C. Naud, P. Mallet, J.-Y. Veuillen, C. Berger, E. H. Conrad, et al., *Phys. Rev. Lett.* **99**, 126805 (2007).
  - [24] A. Mattausch and O. Pankratov, *Phys. Rev. Lett.* **99**, 076802 (2007).
  - [25] J. Soltys, J. Piechota, M. Lopuszynski, and S. Krukowski, arXiv:1002.4717v2 (2010).
  - [26] S. Grimme, *J. Comput. Chem.* **27**, 1787 (2006).